Desalination and Water Treatment
www.deswater.com
doi: 10.5004/dwt.2020.26459

208 (2020) 227–238
December

Filtration efficiency of self-cleaning drum-shaped mesh continuous filter

Hongfei Tao*, Yang Zhou, Wenxin Yang, Mahemujiang·Aihemaiti, Qiao Li, Youwei Jiang, JianQun Wei

College of Water Conservancy and Civil Engineering, Xinjiang Agricultural University, Urumqi 830052, China, Tel. +86 991 8763365; emails: 304276290@qq.com (H.F. Tao), 1712528255@qq.com (Y. Zhou), 314728370@qq.com (W.X. Yang), 1027903576@qq.com (M. Aihemaiti), qiaoli_xjau@qq.com (Q. Li), 240892970@qq.com (Y.W. Jiang), 442829526@qq.com (J.Q. Wei)

Received 20 February 2020; Accepted 14 August 2020

ABSTRACT

Adopting the physical model test method, the filter properties of the self-cleaning drum-shaped mesh continuous filter were measured. The relationships between filtration efficiency and various parameters were explored using dimensional analysis and multiple regression analysis. According to the results, the following statements can be made: (1) under the same influent suspended solids concentration and different flow rates, the effluent suspended solids concentration showed various stages of rapid increase, rapid decrease, slow decrease, and gradual stabilization with time. A higher flow rate caused a faster stabilization of effluent suspended solids concentration and resulted in higher initial and peak effluent suspended solids concentration. (2) Under the same flow rate and different influent suspended solids concentration, the effluent suspended solids concentration showed various stages of rapid increase, rapid decrease, and slow decrease with time. The effluent suspended solids concentration increased with the increase of influent suspended solids concentration. Higher influent suspended solids concentration increased the difficulty for effluent suspended solids concentration stabilization. (3) With the increase of influent suspended solids concentration, the mean filtration efficiency presented a trend in which it first increased and then decreased. (4) A multiple linear regression model was developed for the relationships between mean filtration efficiency and flow rates, influent suspended solids concentration, and drum-shaped mesh rotation speed (correlation coefficient of $R = 0.978$). The model was verified using measured data. The maximum relative error between the predicted and measured values of the mean filtration efficiency was 3.91%, and so, the model can predict the mean filtration efficiency of the filter. The results can provide a theoretical basis and technical support for the structural optimization and management operation of filters.

Keywords: Filter; Filtration efficiency; Flow rates; Suspended solids concentration; Drum-shaped mesh rotation speed

1. Introduction

Agricultural is the biggest consumer of water in the world. Drip irrigation has many advantages over surface irrigation and is widely used in arid and semi-arid areas of the world. Keller and Bliesner [1] reported that the clogging of drip emitters is the biggest maintenance problem of drip irrigation systems. It is difficult to detect when emitters become clogged, and it is expensive to clean or replace them [2].

Water quality is a critical factor in the operation of drip irrigation systems. The causes of emitter clogging can be categorized as physical clogging, chemical clogging, and microbial clogging. In fact, clogging is a combination of these causes. The main clogging problems are caused by suspended particles in irrigation water [3]. Filters are the most

* Corresponding author.

important components in drip irrigation systems, especially when they are used to remove high levels of suspended solids from surface water.

The three common filter types used in drip irrigation systems are sand filters, disc filters, and screen filters [1,4]. Trooien and Hills [5] showed that the standard filtration protection for drip irrigation systems is sand filters. Adin and Alon [3] and Puig-Bargués et al. [6] and Duran-Ros et al. [7,8] and Tripathi et al. [9] and Zeier and Hills [10] reported that screens and disc filters can be used to remove both inorganic particles and suspended organic particles. Generally, different types of filters can be combined to achieve better filtration performance. For example, screen filters or disc filters are often placed after sand filters. Screen filters are simple to operate, convenient to clean, and have higher removal efficiency of inorganic contaminants [11]. Therefore, screen filters are one of the most commonly used filters in drip irrigation systems. The hydraulic performance of screen filters in drip irrigation systems that use municipal effluents has also been studied by several researchers.

Dimensionless analysis and dimensionless parameters are useful tools for the analysis of hydraulic problems. Puig-Bargués et al. [12] developed an equation for calculating the head loss in effluent filtration and adjusted it to provide satisfactory agreement with experimental data. Yurdem et al. [13] developed a mathematical model using dimensional analysis to predict head losses in disc filters, and the experimental head loss data of 12 filters were considered in the model. The predicted value of the head loss is in good agreement with the measured value, and the correlation coefficient is 99.5%. Duran-Ros et al. [14] used dimensional analysis to derive several equations for calculating the head loss of filters that are commonly used in micro-irrigation systems and validated the equations that were established by Puig-Bargués et al. [12] and Yurdem et al. [13] with experimental data. The variables involved in this equation are filtration velocity, the concentration of total suspended solids in the filter influent, total head loss, water density, water viscosity, and inside diameters of the inlet and outlet pipes. It was also noted that it is important to continuously monitor water quality. Yurdem et al. [15] developed mathematical models for predicting the head loss of clean water in hydro cyclone filters that are used in drip irrigation systems. A comparison of different models shows that the models in this study provide better predictions. Elbana et al. [16] developed a new mathematical model for calculating the head loss in a sand filter, and the developed model was compared with the models developed by Puig-Bargués et al. [12] and Duran-Ros et al. [14]. Newly developed and previously developed models are sufficient for calculating the head loss of sand filters. Wu et al. [17] developed a head loss model of screen filters with dimensional analysis; this model included the inner diameter of the inlet/outlet, the angle between the filter body and the inlet/outlet, the diameter of the filter pore, the mesh number, the water velocity of the inlet/outlet, and the average water velocity of filter pore. The correlation coefficient (R) between the measured and predicted values is 0.97. Zong et al. [18] established a head loss equation for self-cleaning screen filters using dimensional analysis; this model considered the parameters that affect head loss included filtration level, total filtration surface, flow rate, the concentration of total sand, filtration time, inside diameter of the inlet and outlet pipes, mean filtration velocity, mean diameter of sand particle size distribution, water viscosity and water density. The regression coefficient of the equation developed in this study is highly significant, and it indicates that it is feasible to use a single equation to calculate the head loss.

Currently, most of the filters that are used in agricultural micro-irrigation are installed behind the pump, and this has the disadvantages of a large head loss, large energy consumption, and high operating costs. Considering the shortcomings of existing filters, this study designed a self-cleaning drum-shaped mesh continuous filter. The aim was to achieve energy savings, emission reductions, cost reductions, and high-efficiency filtration. The self-cleaning drum-shaped mesh continuous filter is a screen filter that is installed before the pump. The role of the suction pump is to move the head from the free level of the sedimentation tank to the centerline of the connecting pipe. The potential energy of the water that flows at the end of the sedimentation tank is used to impact the blades, driving the mesh cylinder to rotate and thereby achieving the filtration of the sandy water flow. The water that is filtered by the filter is pumped into the piping system by another pump for irrigation. At present, a utility model patent [19] (Patent No.: ZL201820770880.4) has been obtained for this product. Previous researchers have extensively studied the filters installed after the pump and have obtained fruitful results. However, in contrast to previous studies, the filter used in this study was installed before the pump and relied on the water flow to drive the rotation of the mesh cylinder. The filtration method used in this study is very different from when the filter is installed after the pump. Therefore, an experimental study of the filtration performance of this filter when it is installed before the pump is needed.

The filtration efficiency is an important parameter for evaluating the filter performance, and it is crucial for the structural design and performance optimization of the filter. In this study, the changes in filtration efficiency with respect to time are discussed by testing the self-cleaning drum-shaped mesh continuous filter under different working conditions. In addition, a mathematical model for predicting the mean filtration efficiency was developed, providing some ideas on how to further improve filter performance and to optimize the filter.

2. Materials and methods

2.1. Dimensional analysis

For complex physical processes, identifying the exact solution to a problem through mathematical reasoning and calculation can be difficult and burdensome. Buckingham's [20] π theorem requires that the relevant nonredundant variables that affect a physical system must be identified. First, the relevant variables that can explain a physical phenomenon must be determined. In previous studies, researchers identified a number of variables that have an effect on the filter [10,12,17,18]. The experimental variables were selected in this study on the basis of the results from previous studies. This study considered 11 parameters that

affect the performance of the filter, including mesh pore size (Φ), flow rate (Q), influent suspended solids concentration (S), water density (ρ), water dynamic viscosity coefficient (μ), acceleration of gravity (g), total effective screen filtration area (A), filtration efficiency (η), drum-shaped mesh rotation speed (n), drum-shaped mesh length (L), and drum-shaped mesh diameter (D), as shown in Table 1.

Many factors may affect hydraulic and filtration performance. On the basis of dimensional analysis, the functional relationship between filtration efficiency and various physical quantities can be obtained, as shown in Eq. (1):

$$f\left(\Phi,Q,S,\rho,\mu,g,A,\eta,n,L,D\right)=0 \tag{1}$$

The π theorem in the dimensional analysis method was used for analysis. All of the variables (m = 11) and their dimensions of length (L), mass (M), and time (T) were considered. The range of the phenomenon dimensional matrix was r = 3. Therefore, there must be 11–3 = 8 π dimensionless groups that can explain the experimental phenomenon, where π_i is a dimensionless group. In this way, the relationship between filtration efficiency and various influencing parameters can be expressed by the functional relationship between the eight dimensionless parameters (π_i).

These dimensionless parameters are as follows:

$$\pi_1=\frac{\rho}{s} \tag{2}$$

$$\pi_2=\frac{\mu\Phi}{QS} \tag{3}$$

$$\pi_3=\frac{g\Phi^5}{Q^2} \tag{4}$$

$$\pi_4=\frac{A}{\Phi^2} \tag{5}$$

$$\pi_5=\eta \tag{6}$$

$$\pi_6=\frac{n\Phi^3}{Q} \tag{7}$$

$$\pi_7=\frac{L}{\Phi} \tag{8}$$

$$\pi_8=\frac{D}{\Phi} \tag{9}$$

Considering these eight π dimensionless groups, Eq. (1) can be expressed as the following function:

$$\eta=f\left(\frac{\rho}{s},\frac{\mu\Phi}{QS},\frac{g\Phi^5}{Q^2},\frac{A}{\Phi^2},\frac{n\Phi^3}{Q},\frac{L}{\Phi},\frac{D}{\Phi}\right) \tag{10}$$

Table 1
Main parameters of dimensional analysis

	Φ	Q	S	ρ	μ	g	A	η	n	L	D
M	0	0	1	1	1	0	0	0	0	0	0
L	1	3	–3	–3	–1	1	2	0	0	1	1
T	0	–1	0	0	–1	–2	0	0	–1	0	0

To prove the validity of the dimensionless parameters included in the above equations, an experimental method was employed to obtain the unknown parameters.

2.2. Experimental device

The experiments were conducted at the Laboratory of Agricultural Water Conservancy Engineering of the College of Water Conservancy and Civil Engineering at the Xinjiang Agricultural University. Fig. 1 shows the experimental apparatus, which consists of a mixing tank (67.5 cm × 46 cm × 35.5 cm), filtered water tank (60.5 cm × 42.5 cm × 51 cm), sand collection tank (22 cm × 42.5 cm × 51 cm), suction pump, filter, inlet/outlet pipes, and valves.

Before the sand water mixture experiment, tap water and sand were injected into the mixing tank until the desired concentration was reached. The proportion of sand was 37.66% for sand that was less than 0.25 mm and 97.15% for sand that was less than 0.5 mm. Then, the water and sand were uniformly mixed using a mixing device before the experiment was started. During the experiment, the water in the mixing tank was pumped by the suction pump through an inlet pipe of the mixing tank into the filter. After filtration by the filter, the water flowed into the filtered water tank. Next, the filtered water was pumped by a circulating pump back into the mixing tank. Finally, driven by the suction pump, the water in the mixing tank flowed into the filter for filtration. The whole experimental apparatus can be approximated as a circulating filtration system.

2.3. Experimental scheme

The experiments were conducted at room temperature (26°C–28°C) with a water temperature of approximately 23°C. The experimental groups were scheduled following the comprehensive experimental method. The experiments adopted five flow rates (1.2, 1.7, 2.4, 3.0, and 3.5 m^3/h) and five influent suspended solids concentration (0.5, 0.8, 1.2, 1.5, and 2.5 g/L). Table 2 shows the details of the experimental groups. The influent suspended solids concentration and flow rate were taken as the main factors that affect the filtration efficiency and drum-shaped mesh rotation. At the beginning of the experiment, a uniform mixture of water and sand was added into the mixing tank. In addition, sandy water samples were collected from the outlet at regular intervals. Samples have been collected a total of eight times in each test. At the end of the experiment, all of the sandy water samples were tested. The filtration efficiency of the filter under different operating conditions was analyzed by measuring the variations in the effluent suspended solids concentration under different experimental

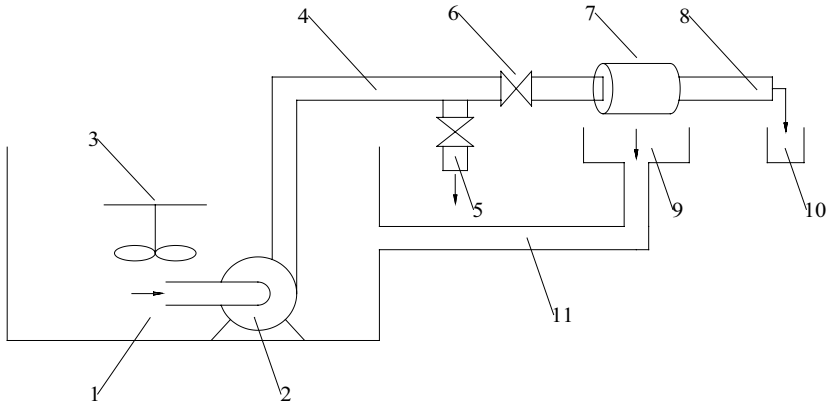

Fig. 1. Schematic diagram of the experimental apparatus. (1) Mixing tank; (2) suction pump; (3) mixture device; (4) inlet pipe; (5) flow regulating valve; (6) flow rate valve; (7) filter; (8) sand outlet; (9) filtered water tank; (10) sand collection tank; (11) circulating water pipe.

Table 2
Experimental groups

Experiment	Screen mesh	Influent flow Q (m^3/h)	Influent suspended solids concentration S (g/L)	Filtration time T (s)
Net barrel rotation	80	1.2	0.5	1,200
		1.7	0.8	
		2.4	1.2	
		3.0	1.5	
		3.5	2.5	

conditions. To shorten the experimental duration and to observe obvious experimental phenomena, coarse sand was used for the experiments at high influent suspended solids concentration. Fig. 2 shows the particle size distribution of the sand samples that were used in the turbid water experiment, that is, d_{50} = 0.315 mm. Currently, 80 and 120 mesh screen filters are most commonly used for agricultural micro-irrigation. This study mainly investigated the filtration efficiency of an 80 mesh screen filter under different experimental conditions.

3. Results and analysis

3.1. Effluent suspended solids concentration variation under the same influent suspended solids concentration and different flow rates

The filtration performance of the filter was investigated. Experiments were carried out under the same influent suspended solids concentration condition, and effluent suspended solids concentration was measured for five different influent flow rates. Thus, the variation curve of effluent suspended solids concentration with respect to time under the same influent suspended solids concentration and different flow rates were plotted, as illustrated in Fig. 3. The following main conclusions can be drawn from Fig. 3:

- Within a filtration time of 1,200 s, the variation of effluent suspended solids concentration with respect to time under the same influent suspended solids concentration and different flow rates can be roughly divided into four stages, that is, rapid increase, rapid decrease, slow decrease, and gradual stabilization. When the influent suspended solids concentration was between 0.5 and 1.5 g/L and different influent flow rates were adopted, there were four stages, as shown in Figs. 3a–d. With the extended filtration time, the effluent suspended solids concentration exhibited a trend that first increased and then decreased. At 40–120 s, the effluent suspended solids concentration quickly reached its peak value and then rapidly decreased. At about 900 s, the concentration tended to stabilize. As seen in Fig. 3e, when the influent suspended solids concentration was 2.5 g/L, there was no stabilization stage. This is because, at different flow rates, the volumes of sand water samples treated by the filter within each time unit differed as well, resulting in different effluent suspended solids concentrations.
- Under the same influent suspended solids concentration, higher flow rates resulted in a higher initial and peak effluent suspended solids concentration. The initial effluent suspended solids concentration was far lower than the peak effluent suspended solids concentration. As seen in Fig. 3b, when the flow rate was 1.2 m^3/h, the initial and peak effluent suspended solids concentrations were 0.04 and 0.12 g/L, respectively. When the flow rate was 3.5 m^3/h, they were 0.08 and 0.22 g/L, respectively. This is because, under a given influent suspended solids concentration, the increase in the flow rate would

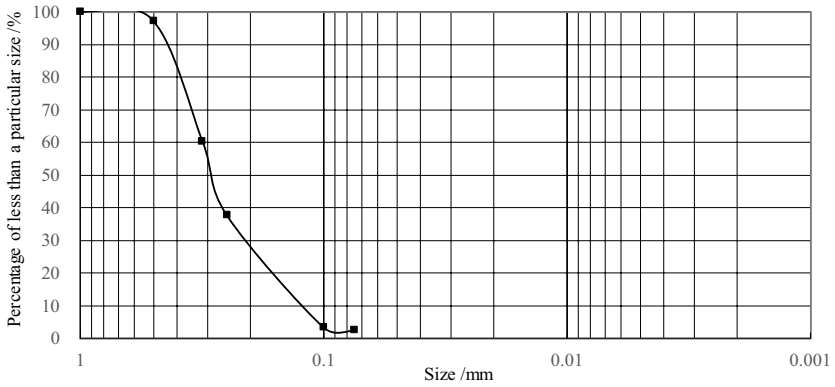

Fig. 2. Grain-size distribution of sand.

increase the amount of sand particles on each filter screen unit. Consequently, this would increase the initial and peak effluent suspended solids concentrations.

- The flow rate exerted a great effect on effluent suspended solids concentration. When the flow rate was low, the effluent suspended solids concentration varied slowly with time, whereas with an increase in flow rate, it presented an abruptly decreasing trend. The increase in flow rate shortened the duration of the variation process of the effluent suspended solids concentration. In particular, the effluent suspended solids concentration varied dramatically within a short period of time and quickly reached a stable value. As seen in Fig. 3c, when the flow rate increased from 1.2 to 3.5 m^3/h, a low stable value of effluent suspended solids concentration (0.02 g/L) was reached before 600 s. This was mainly because of the limited influent suspended solids concentration in the tank. That is, when the flow rate increased, the filter would treat more suspended particles within each time unit. In this case, the effluent suspended solids concentration would decrease to a stable value more quickly.

3.2. Effluent suspended solids concentration variation under the same flow rate and different influent suspended solids concentrations

The experiments were conducted under the same influent flow rate, and the effluent suspended solids concentrations were measured for five influent suspended solids concentration. Thus, the variation curve of effluent suspended solids concentration with respect to time under the same flow rate and different influent suspended solids concentrations were plotted, and the results are shown in Fig. 4. The following main conclusions can be drawn from Fig. 4:

- Under the same flow rate and different influent suspended solids concentrations, the variation curve of effluent suspended solids concentration with respect to filtration time can be roughly divided into three stages, that is, rapid increase, rapid decrease, and slowly decrease. When the flow rate was 1.2–2.4 m^3/h, the effluent suspended solids concentration reached its peak value in the range of 60–120 s and tended to stabilize at 1,200 s. When the flow rate increased to 3.0–3.5 m^3/h, it reached its peak value in the range of 40–60 s, and then it tended to stabilize at 900 s (except for the case where the influent suspended solids concentration was 2.5 g/L). This is mainly because high influent suspended solids would make filter treatment more difficult. This would make it very hard for the effluent suspended solids concentration to decrease to a stable value within a short period of time.
- Under the same flow rate, the effluent suspended solids concentration increased with an increase in the influent suspended solids concentration. A lower influent suspended solids concentration would ease the stabilization of effluent suspended solids concentration. As seen in Fig. 4e, when the influent suspended solids concentration was 0.5 g/L, the effluent suspended solids concentration reached a stable value (0.02 g/L) at 240 s. When the influent suspended solids concentration was increased to 2.5 g/L, the effluent suspended solids concentration reached 0.1 g/L at 1,200 s. More specifically, when the water source had a lower influent suspended solids concentration, the treatment was easier, which is consistent with engineering practice. This is because the increase in the influent suspended solids concentration increases the amount of suspended solid particles entering the filter within each time unit, speeds up mesh clogging, and reduces filtration efficiency. As a result, this increases the effluent suspended solids concentration and prolongs the time needed for the effluent suspended solids concentration to stabilize.
- The influent suspended solids concentration exerted an important effect on the effluent suspended solids concentration. With an increase in the influent suspended solids concentration, the peak of the effluent suspended solids concentration rose, whereas the effluent suspended solids concentration declined at a slower pace. The increase in the influent suspended solids concentration also extended the length of time during which the effluent suspended solids concentration varies. As a result, because the effluent suspended solids concentration varied slowly over a long period of time, it was more difficult to stabilize. As shown in Fig. 4a, when the influent suspended solids concentration was increased from 0.5 to 2.5 g/L, the peak effluent

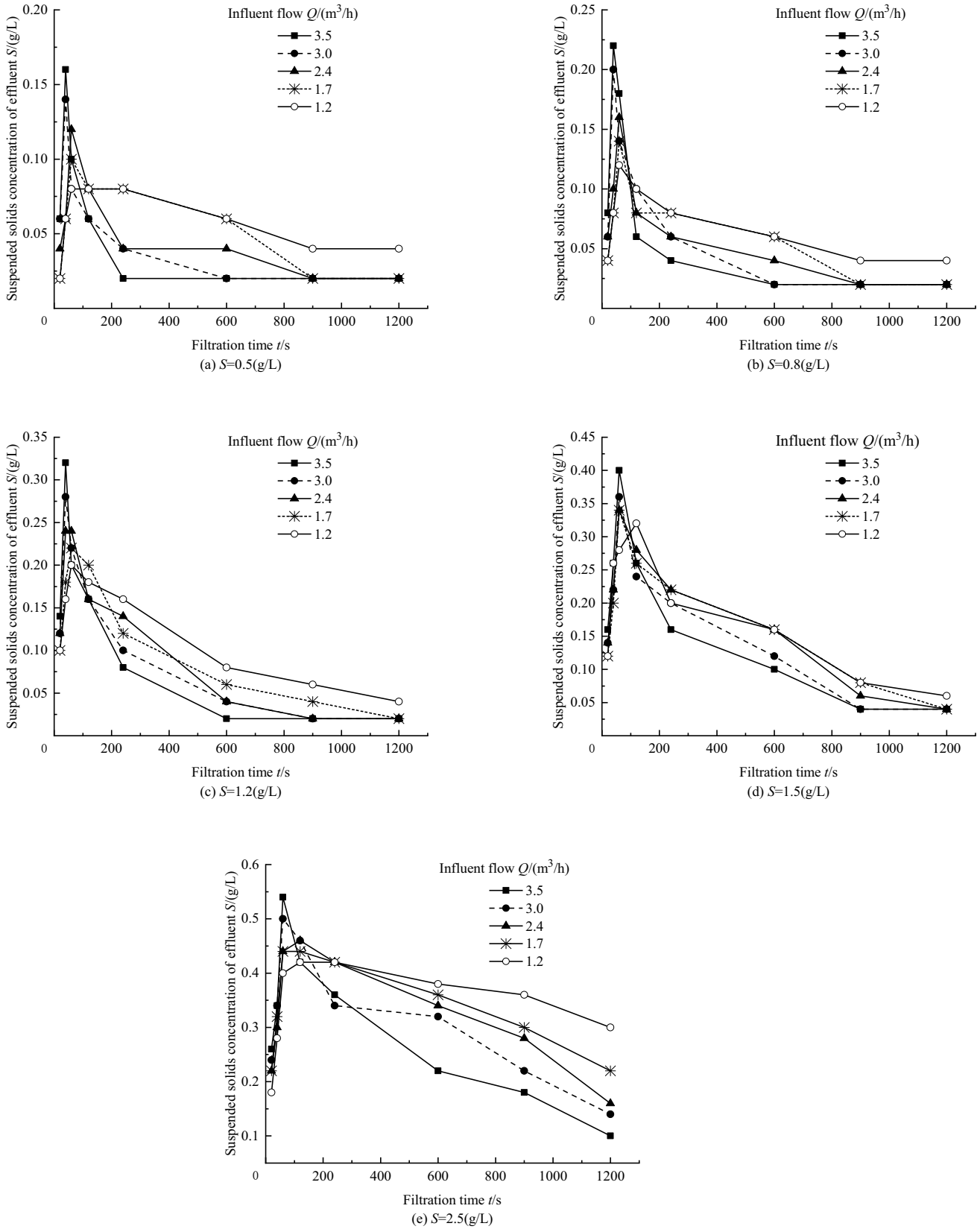

Fig. 3. Variation curves of effluent suspended solids concentration with filtration time under the same influent suspended solids concentration and different flow rates (a) S=0.5(g/L), (b) 0.8(g/L), (c) 1.2(g/L), (d) 1.5(g/L), (e) 2.5(g/L).

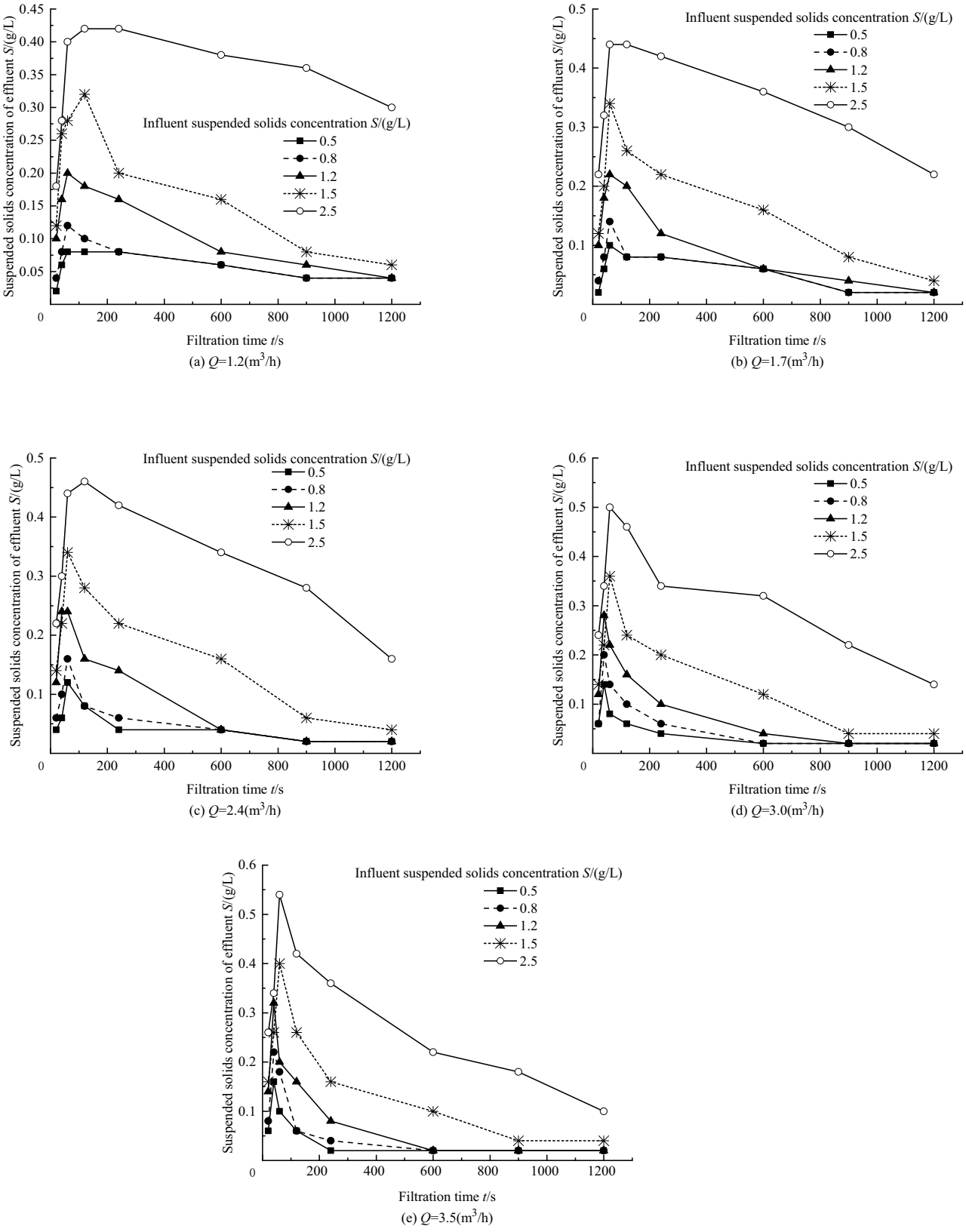

Fig. 4. Variation curves of effluent suspended solids concentration with respect to filtration time under the conditions of the same flow rate and different influent suspended solids concentrations (a) Q=1.2(m^3/h), (b) 1.7(m^3/h), (c) 2.4(m^3/h), (d) 3.0(m^3/h), (e) 3.5(m^3/h).

suspended solids concentration increased from 0.08 to 0.42 g/L. When the filtration time was 1,200 s, the corresponding effluent suspended solids concentration was 0.04 and 0.3 g/L, respectively. The main reason is that the increase of influent suspended solids concentration increased the amount of suspended solids concentration particles contained in each unit of volume in the tank. When the flow rate remained constant, the amount of suspended solid particles entering the filter within each time unit would increase, thus increasing the probability and area of screen clogging. Consequently, this increases the effluent suspended solids concentration, which stabilizes with difficulty. In engineering practice, the filtration efficiency and filtration rate of the filter should be comprehensively considered in the selection of a suitable flow rate to give full play to the sand treatment capacity of the filter.

The flow rate was found to have an important effect on the rate of stabilization of the effluent suspended solids concentration. Under a given influent suspended solids concentration, when the flow rate was higher, the effluent suspended solids concentration stabilize faster. This is mainly because of the special structural form of the filter and the recirculating effect. That is, the filter adopts the water-driven mode to provide a power source for drum-shaped mesh rotation. Therefore, the suspended solids concentrations inside the drum-shaped mesh are mainly under the combined effects of gravity and centrifugal force. In this study, under a given influent suspended solids concentration, a higher flow rate generated a higher drum-shaped mesh rotation speed, causing more serious damage to the surface bonding between particles and the drum-shaped mesh. When suspended solids particle groups were rolled on the inner surface of the drum-shaped mesh, they imposed a shearing sweep flow effect on the inner surface. In addition, they restricted the formation and thickening of the cake layer and delay mesh clogging, thereby improving filtration efficiency and extending the filtration cycle.

3.3. Filtration efficiency analysis

Samples of suspended solids were extracted in each experimental stage. Eight quantitative samples were collected in each experiment, filtered through filter paper, and weighed after drying to calculate the suspended solids concentration. The filtration efficiency can be calculated by Eq. (11):

$$\eta = \frac{S - S_1}{S} \times 100\% \tag{11}$$

where η is the filtration efficiency (%), S is the influent suspended solids concentration (g/L), and S_1 is the effluent suspended solids concentration (g/L).

The data of the turbid water experiment were substituted into Eq. (11) to calculate the minimum and mean filtration efficiencies under different working conditions. As shown in Table 3, under a given influent flow rate, with an increase in influent suspended solids concentration, the mean filtration efficiency presented a trend that first increased and then decreased. This is because the increase in the influent suspended solids concentration increases the probability and extent of screen clogging, thus reducing the filtration efficiency.

Under a given influent suspended solids concentration, the mean filtration efficiencies under different flow rates were pretty close, whereas the minimum filtration efficiencies were significantly different. For instance, when the influent suspended solids concentration was 1.2 g/L, the maximum difference in mean filtration efficiency was only 0.4%, whereas that in the minimum filtration efficiency was 10%. Under low flow rates (1.2–3.0 m^3/h), the minimum filtration efficiency showed a trend that first increased, then decreased, and then increased again. Under the maximum flow rate (3.5 m^3/h), it increased with an increase in the influent suspended solids concentration. Under the condition of influent suspended solids concentration of 2.5 g/L and flow rate of 3.5 m^3/h, the filter had a minimum filtration efficiency of 87.4%, which was only 0.5% different from the mean filtration efficiency. This suggests that the filter had high filtration efficiency and stable filtration performance under this working condition.

3.4. Multiple regression analysis

3.4.1. Filtration efficiency model development

The experimental data were arranged according to Eq. (11) to obtain the filtration efficiency (η_{mean}) and other relevant parameters under different working conditions. Fifteen groups of data with influent suspended solids

Table 3
Filtration efficiency under different conditions

Flow rate (m^3/h)	Influent suspended solids concentration (g/L)									
	0.5		0.8		1.2		1.5		2.5	
	η_{mean} (%)	η_{min} (%)	η_{mean} (%)	η_{min} (%)	η_{mean} (%)	η_{min} (%)	η_{mean} (%)	η_{min} (%)	η_{mean} (%)	η_{min} (%)
1.2	88.5	84.0	91.3	85.0	89.8	83.3	87.7	78.7	86.3	83.2
1.7	89.0	80.0	91.9	82.5	90.2	81.7	88.2	77.3	86.4	82.4
2.4	89.5	76.0	91.6	80.0	89.8	80.0	87.8	77.3	86.9	81.6
3.0	89.0	72.0	90.3	75.0	90.0	76.7	88.7	76.0	87.2	80.0
3.5	88.5	68.0	90.0	72.5	90.0	73.3	88.2	73.3	87.9	87.4

concentration (S) of 1.2–2.5 g/L were selected for multiple regression analysis.

The data from the physical parameters of the filter and water were used to calculate the different dimensionless groups. After logarithmic conversion, multiple linear regression analysis was performed on the dimensionless parameters using SPSS statistical software. The regression standardized residual plot shows that the data are distributed along the diagonal direction (Fig. 5). The regression model satisfies the normality hypothesis and can be used for regression analysis. The statistical significance level was set as 0.05, and a parameter was excluded if $P > 0.1$, indicating that the parameter has no significant effect on the experiment results.

By applying Eq. (10), the following equation can be obtained:

$$\eta_{mean} = a\left(\frac{\rho}{S}\right)^{k_1}\left(\frac{\mu\Phi}{QS}\right)^{k_2}\left(\frac{g\Phi^5}{Q^2}\right)^{k_3}\left(\frac{A}{\Phi^2}\right)^{k_4}\left(\frac{n\Phi^3}{Q}\right)^{k_5}\left(\frac{L}{\Phi}\right)^{k_6}\left(\frac{D}{\Phi}\right)^{k_7} \quad (12)$$

where a is an empirical coefficient, and k_1, k_2, k_3, k_4, k_5, k_6 and k_7 are empirical exponents.

The statistical analysis results of the newly established model are shown in Table 4. The independent variables π_4, π_7, and π_8 had no significant unstandardized coefficients ($P > 0.1$). Therefore, these parameters have no statistically significant effects on the studied phenomenon and were excluded from the developed model. The independent variables π_1, π_2, π_3, and π_6 all have significant effects on the studied phenomenon ($P < 0.1$). From the magnitude of the standardization coefficients, the influences that the independent variables have on the dependent variables are in the following order: π_2, π_3, π_1, and π_6.

The values of the empirical coefficients, exponents, and determination coefficient of Eq. (9) are shown in Table 4. The exponents k_1, k_2, and k_3 are all significant ($P < 0.001$). Although the significance level of k_5 is greater than 0.05, it is still included in the model to investigate the effect it has on the filtration efficiency. Some π terms that were obtained from certain geometric variables are constant for each specific filter, and thus, the exponents k_4, k_6, and k_7 are zero. The new mathematical model of filtration efficiency is defined by Eq. (13):

$$\eta_{mean} = e^{4.704}\left(\frac{\rho}{S}\right)^{-0.201}\left(\frac{\mu\Phi}{QS}\right)^{0.285}\left(\frac{g\Phi^5}{Q^2}\right)^{-0.145}\left(\frac{n\Phi^3}{Q}\right)^{0.012} \quad (13)$$

Eq. (13) can be simplified, and the model for predicting filtration efficiency can be written as follows:

$$\eta_{mean} = e^{4.704}\rho^{-0.201}\mu^{0.285}g^{-0.145}S^{-0.084}\Phi^{-0.404}Q^{-0.007}n^{0.012} \quad (14)$$

The fitted correlation coefficient (R) could reach 0.978, suggesting that the equation had the goodness of fit. It is assumed that the water temperature in the experimental process was constant (23°C). By substituting the standard values of water density (ρ), dynamic viscosity coefficient of water (μ), acceleration of gravity (g), and mesh pore size (Φ) into Eq. (14), the mathematical model for predicting filtration efficiency can then be written as follows:

$$\eta_{mean} = 88.06S^{-0.084}Q^{-0.007}n^{0.012} \quad (15)$$

where Q is the flow rate (m^3/s), S is the influent suspended solids concentration (g/L), and n is the drum-shaped mesh rotation speed (r/s).

According to Eqs. (14) and (15), under the condition that the experimental temperature, experimental site, and number of filter mesh are determined, the mean filtration efficiency of the filter is related to the structural characteristics and operating conditions of the filter. The change in mean filtration efficiency is mainly the result of the combined effects of flow rate, influent suspended solids concentration, and drum-shaped mesh rotation speed. The model gives satisfactory results within the range of the related variables that were tested.

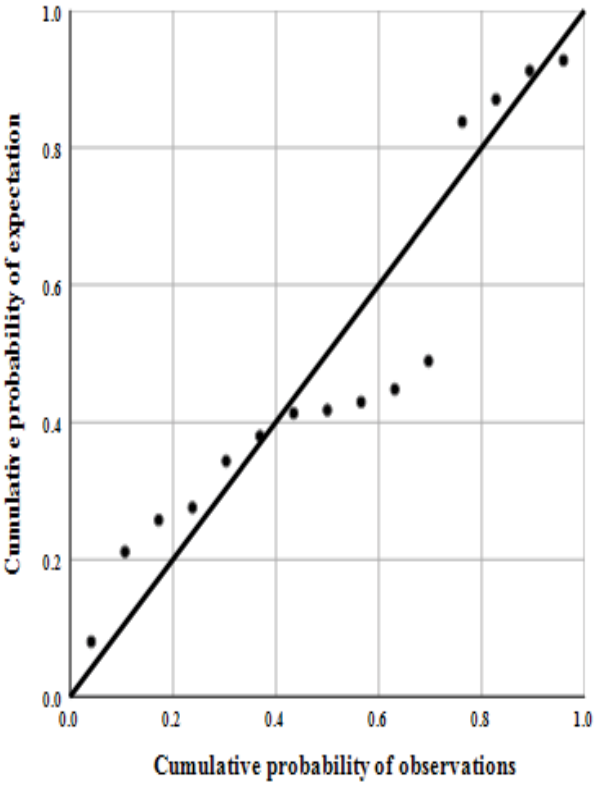

Fig. 5. Normal P–P plot of regression standardized residuals.

3.5. Comparison of measured and predicted filtration efficiency

By substituting the experimental data of influent suspended solids concentration, flow rate, and the drum-shaped mesh rotation speed into Eq. (15), the predicted value of the mean filtration efficiency can be obtained and compared with the measured value. As seen in Fig. 6, under the same conditions, the predicted values were distributed around the measured values. This suggests that they were very close to each other. The prediction of the model has a certain degree of error, and therefore, in some cases, the predicted

Table 4
Statistical analysis results for the model

Dependent variable	*P*-level	R^2	Independent variables	Unstandardized coefficients		Standardized coefficients	Root-mean-square error
				B	Standard error		
$\ln\pi_5$	<0.001	0.956	Constant	4.704	0.156		0.004
			$\ln\pi_1$	–0.201[a]	0.044	–5.170	
			$\ln\pi_2$	0.285[a]	0.055	9.564	
			$\ln\pi_3$	–0.145[a]	0.028	–7.593	
			$\ln\pi_6$	0.012[b]	0.006	0.214	

[a]Probability $p \le 0.001$;
[b]Probability $p < 0.1$.

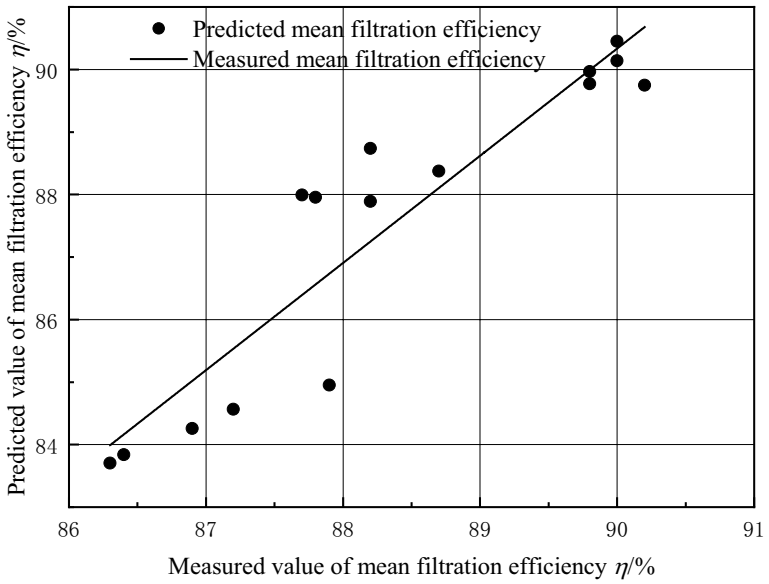

Fig. 6. Comparison of measured and predicted mean filtration efficiency.

results are too high or too low. The correlation coefficient (*R*) is 0.92 between the measured and predicted values, and this indicates that the prediction was relatively good. This suggests that using the influent suspended solids concentration, flow rate, and drum-shaped mesh rotation speed to predict the variations of mean filtration efficiency helps to simplify the analysis process. Furthermore, it indicates that the model has certain reliability in predicting the mean filtration efficiency of the filter.

4. Discussion

In the study reported by Puig-Bargués et al. [12], there are 6 variables (filtration level (ϕ_f), total filtration surface (*A*), flow rate across the filter (*Q*), the concentration of total suspended solids (*C*), water viscosity (μ), and the water density (ρ) in common with the selected model in this study. Some parameters that are not considered in this study were taken into account in their studies, such as the mean diameter of the effluent particle size distribution (D_p), water volume across the filter (*V*), and head loss across the filter (Δ*H*). Similarly, the model established by Duran-Ros et al. [14] has five variables in common with the model established in this study (total filtration surface, the concentration of total suspended solids, water viscosity, water density, and filtration level). Two other parameters were used in their developed model (filtration velocity and inside diameter of the inlet and outlet pipe). Elbana et al. [16] used the following parameters to describe the head loss of the sand filter: sand effective diameter (d_e), suspended solids average concentration (*C*), acceleration due to gravity (*g*), water density (ρ), water volume (*V*), and internal sand filter diameter (d_f). Wu et al. [17] included the structural parameters of the filter and the parameters of the filter medium in their model. The parameters included in Wu's model are the inner diameter of the inlet/outlet (D_p), angle (α), filter mesh diameter (d_m), mesh number (*M*), water velocity (V_i), average water velocity of the filter pore (V_m), water density (ρ), gravity (*g*), water viscosity (μ), and heat loss (Δ*H*). In the studies reported by Puig-Bargués et al. [12], Duran-Ros et al. [14], Elbana et al. [16], and Wu et al. [17], the treated water came from different

Table 5
Comparison of measured and predicted mean filtration efficiency

Working condition	η (%) Measured value	Flow rate Q (m^3/h)	Influent suspended solids concentration S (g/L)	Drum-shaped mesh rotation speed n (r/s)	Predicted value η (%)	Relative error (%)
1	90.0	3.5	0.8	0.55	93.52	3.91%
2	90.3	3.0	0.8	0.4166	93.31	3.33%
3	91.6	2.4	0.8	0.3166	93.14	1.69%
4	91.9	1.7	0.8	0.1833	92.76	0.93%
5	91.3	1.2	0.8	0.1667	92.88	1.73%

sources, and a mathematical model for the head loss was established. However, these models have different constant values and exponents, and these differences can be explained by differences in the experimental conditions used in different studies.

There are many mathematical models for calculating head loss for different types of filters; however, there are few mathematical models for filter filtration efficiency. Therefore, in this study, a mathematical model for filtration efficiency was developed. However, the variables and research objectives for calculating head loss and for modeling filtration efficiency are not the same. Therefore, it is impossible to compare the results obtained with the model developed in this study to the results obtained by previous researchers. Therefore, in this study, to validate our model, we used five sets of test samples that were previously reserved used to verify the calculation results of the model.

The experimental data obtained with an influent suspended solid concentration of 0.8 g/L and different flow rates were used to verify the prediction accuracy of the developed model. As shown in Table 5, the mean filtration efficiency decreased gradually with an increase in the flow rate. Also, the maximum relative error between the predicted and measured values of the mean filtration efficiency was 3.91%, whereas the minimum relative error was 0.93%. As shown by the experiments, the flow rate, influent suspended solids concentration, and drum-shaped mesh rotation speed can accurately predict the mean filtration efficiency of the model.

5. Conclusions

- By testing the filter with turbid water, this study identified the various stages of its effluent suspended solids concentration with filtration time; the stages are a rapid increase, rapid decrease, slow decrease, and gradual stabilization. The effluent suspended solids concentration increased with an increase in influent suspended solids concentration. When the influent suspended solids concentration and flow rate were higher, the initial and peak effluent suspended solids concentrations were higher. A higher influent suspended solids concentration made it more difficult for the effluent suspended solids concentration to reach stability. Higher flow rates led to a faster decrease and stabilization of effluent suspended solids concentration.
- The minimum and mean filtration efficiency were calculated for different working conditions. According to the calculation results, with an increase in the influent suspended solids concentration, the mean filtration efficiency presented a trend that first increased and then decreased. The filtration efficiency was most stable under an influent suspended solids concentration of 2.5 g/L and a flow rate of 3.5 m^3/h. Under different working conditions, the minimum mean filtration efficiency of the filter was 86.3%. Moreover, the filter showed a high filtration efficiency and stable filtration performance.
- This study derived the dimensionless parameters that affect the filtration efficiency of a filter based on dimensional analysis. In addition, a mathematical model for predicting the mean filtration efficiency of a filter was established via multiple regression. Model verification was performed using the experimental data, and the verification results showed that the predicted value of the model agrees well with the measured value. Therefore, the model can predict the mean filtration efficiency of the filter well.

Through experimental verification of the model under different working conditions, the parameter range of the model was determined to be as follows: flow rate of 1.2–3.5 m^3/h, influent suspended solids concentration of 0.8–2.5 g/L, and drum-shaped mesh rotation speed of 0.167–0.55 r/s. The model proposed in this study can be used to accurately predict the mean filtration efficiency within the given parameter ranges. The results provide some reference for predicting the mean filtration efficiency of a filter. Further research is needed to verify the applicability of the model in other ranges.

Acknowledgment

This study is financially supported by the Xinjiang Uygur Autonomous Region Special Project for the Construction of Innovative Environment (Talents and Bases) - Natural Science Foundation Project (2020D01B33), Xinjiang Uygur Autonomous Region Special Project for the Construction of Innovative Environment (Talents and Bases) - "Tianshan Youth Plan" Project (2019Q075), Xinjiang Water Resources Engineering Key Discipline Research Project (SLXK2017-01, SLXK2018-05), and Xinjiang Uygur Autonomous Region University Research Plan for Applied Technology and Transformation (Technology Promotion) Project (XJEDU2017A002).

References

[1] J. Keller, R.D. Bliesner, Sprinkle and Trickle Irrigation, AVI Books, New York, 1990.

[2] A. Capra, B. Scicolone, Emitter and filter tests for wastewater reuse by drip irrigation, Agric. Water Manage., 68 (2004) 135–149.
[3] A. Adin, G. Alon, Mechanisms and process parameters of filter screens, J. Irrig. Drain. Eng., 112 (1986) 293–304.
[4] V. Demir, E. Uz, Filters used in drip irrigation systems, The J. Agric. Faculty Ege Univ., 31 (1994) 177–184.
[5] T.P. Trooien, D.J. Hills, Application of Biological Effluent, F.R. Lamm, J.E. Ayars, F.S. Nakayama, Eds., Microirrigation for Crop Production. Design, Operation, and Management, Elsevier, Amsterdam, 2007, pp. 329–356.
[6] J. Puig-Bargués, J. Barragán, F. Ramírez de Cartagena, Filtration of effluents for microirrigation systems, Trans. Am. Soc. Agric. Biol. Eng., 48 (2005) 969–978.
[7] M. Duran-Ros, J. Puig-Bargués, G. Arbat, J. Barragán, F. Ramírez de Cartagena, Effect of filter, emitter and location on clogging when using effluents, Agric. Water Manage., 96 (2009) 67–79.
[8] M. Duran-Ros, J. Puig-Bargués, G. Arbat, J. Barragán, F. Ramírez de Cartagena, Performance and backwashing efficiency of disc and screen filters in microirrigation systems, Biosyst. Eng., 103 (2009) 35–42.
[9] V.K. Tripathi, T.B.S. Rajput, N. Patel, Performance of different filter combinations with surface and subsurface drip irrigation systems for utilizing municipal wastewater, Irrig. Sci., 32 (2014) 379–391.
[10] K.R. Zeier, D.J. Hills, Trickle irrigation screen filter performance as affected by sand size and concentration, Trans. Am. Soc. Agric. Biol. Eng., 30 (1987) 735–739.
[11] J. Puig-Bargués, G. Arbat, J. Barragán, F. Ramírez de Cartagena, Hydraulic performance of drip irrigation subunits using WWTP effluents, Agric. Water Manage., 77 (2005) 249–262.
[12] J. Puig-Bargués, J. Barragán, F. Ramírez de Cartagena, Development of equations for calculating the head loss in effluent filtration in microirrigation systems using dimensional analysis, Biosyst. Eng., 92 (2005) 383–390.
[13] H. Yurdem, V. Demir, A. Degirmencioglu, Development of a mathematical model to predict head losses from disc filters in drip irrigation systems using dimensional analysis, Biosyst. Eng., 100 (2008) 14–23.
[14] M. Duran-Ros, G. Arbat, J. Barragán, F. Ramírez de Cartagena, J. Puig-Bargués, Assessment of head loss equations developed with dimensional analysis for micro irrigation filters using effluents, Biosyst. Eng., 106 (2010) 521–526.
[15] H. Yurdem, A. Degirmencioglu, V. Demir, Development of a mathematical model to predict clean water head losses in hydrocyclone filters in drip irrigation systems using dimensional analysis, Biosyst. Eng., 105 (2010) 495–506.
[16] M. Elbana, F. Ramírez de Cartagena, J. Puig-Bargués, New mathematical model for computing head loss across sand media filter for microirrigation systems, Irrig. Sci., 31 (2011) 343–349.
[17] W.Y. Wu, W. Chen, H.L. Liu, S.Y. Yin, Y. Niu, A new model for head loss assessment of screen filters developed with dimensional analysis in drip irrigation systems, Irrig. Drain, 63 (2014) 523–531.
[18] Q.L. Zong, T.G. Zheng, H.F. Liu, C.J. Li, Development of head loss equations for self-cleaning screen filters in drip irrigation systems using dimensional analysis, Biosyst. Eng., 133 (2015) 116–127.
[19] H. Tao, Self-Cleaning Drum-Shaped Mesh Continuous Filter, CN208406337U, 2019–01–22.
[20] E. Buckingham, Model experiments and the form of empirical equations, Trans Am. Soc. Agric. Biol. Eng., 37 (1915) 263–296.